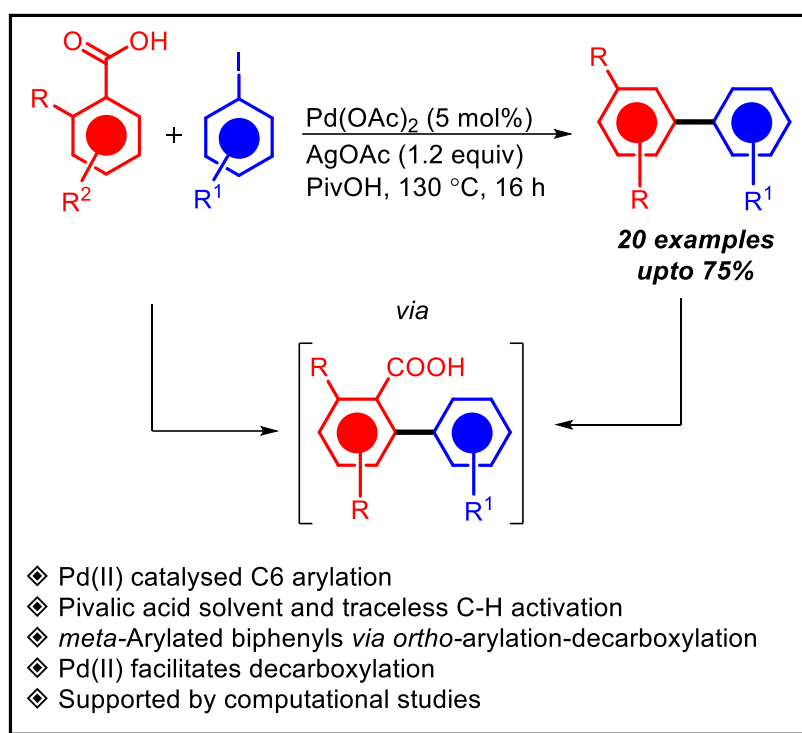


# Chapter 2

## Palladium Catalysed Access to *meta*-Substituted Biphenyls via Carboxylic acid Directed *ortho*-Arylation-Decarboxylation Cascade



**Abstract:** The inherent *ortho*-directing characteristic of the carboxylic acid functional group is harnessed in the traceless C6 arylation of C2-substituted benzoic acids using aryl iodides under palladium catalysis. This results in the formation of *meta*-substituted biphenyls. The process involves a sequential pathway, starting with traceless carboxylate-directed C6 arylation followed by decarboxylation. The use of a bulky protic solvent, such as pivalic acid, eliminates the need for higher quantities of arylating agents compared to earlier methods. Theoretical studies further elucidate the tandem directed arylation-decarboxylation pathway.

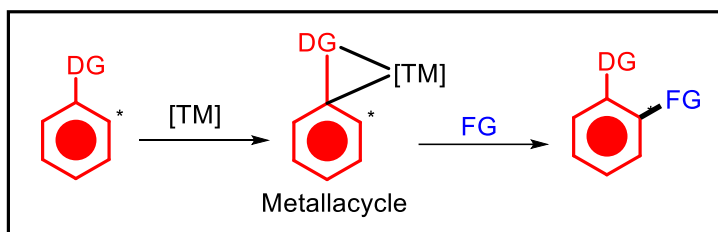
---

## Palladium (II) Catalysed Access to *meta*-Substituted Biphenyls via Carboxylic acid Directed *ortho*-Arylation-Decarboxylation Cascade

### 2.1. Introduction

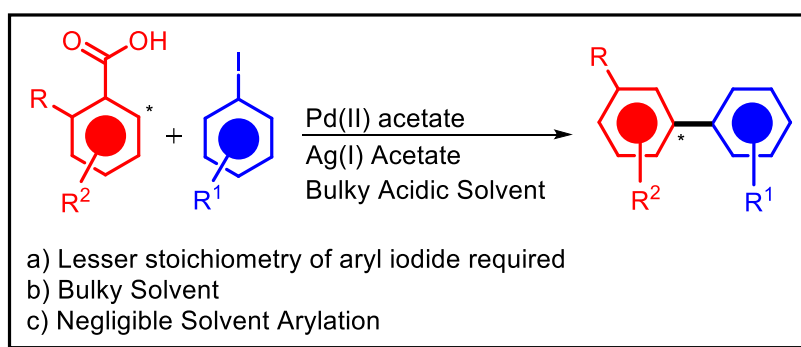
The interest in the synthesis of biaryls has grown significantly owing to the widespread presence of these compounds [1, 2]. Traditional methods, including those relying on transition metal catalysis [3–6, 2] and the Fittig reaction [7–9], often rely on organometallic aryl donors that result in substantial waste generation. Processes introducing aryl groups at *meta*-C-H positions in aromatic compounds typically involve multiple sequential steps, compromising overall efficiency. The emergence of C-H functionalisation strategies has revolutionised direct arylation at aromatic C-H positions, eliminating the need for organometallic aryl donors. Directing moieties like pyridyls, nitriles, amides, carboxylic acids, sulfonamides, amines, ketones, etc., play a pivotal role in facilitating direct *ortho*-arylation processes [10,11]. While achieving selective *meta*-arylations historically posed a challenge due to lower reactivity at the *meta*-position, Gaunt and colleagues achieved a groundbreaking *meta*-arylation of pivaloyl anilines and benzyl Weinreb amides through Cu(II) catalysis, using diaryl iodonium salts as aryating agents. This method was extended to achieve C6 arylation of *N*-pivaloyl indoles [12]. Subsequent contributions by Ackermann, Hartwig, and Frost have expanded the field of *meta*-arylation through novel catalytic systems and innovative protocols [13–15].

Arylations *via* C-H activation assisted by directing groups depend on the initial coordination of the catalytic metal center to the directing group. This brings the directing group into proximity to the target C-H bond, facilitating functionalisation. However, the spatial arrangement of a *meta*-C-H bond presents challenges in forming the desired metallacycle. The incorporation of chain templates at the *ipso*-position, along with a coordinating center at the terminal position (e.g., a nitrile), enables C-H activation at both proximal and distal C-H sites (*meta*- and *para*-positions). This concept, introduced by Yu and collaborators [16], has been further developed by the Yu and Maiti research groups [17–20], resulting in a significant advancement in transformative processes.



**Scheme 2.1.** Transition metal catalysed C-H functionalisation

Larrosa's Pd(II)-catalysed decarboxylative *ortho*-benzoic acid arylation relies on a super-stoichiometric arylating agent (usually aryl iodide) and silver salt to streamline the protodecarboxylation process at an elevated temperature of 130 °C [21]. However, a significant side reaction involves the arylation of acetic acid [22– 24]. Presenting a modified protocol for the arylation of benzoic acids with *ortho* substituents, this method eliminates the need for a super-stoichiometric arylating agent. Instead, a bulky protic acid solvent, like pivalic acid, substitutes smaller solvents such as acetic acid. This modification reduces solvent arylation, yielding *meta*-arylated products with efficiency comparable to the original protocol. Computational studies suggest a tandem process involving traceless carboxylate assisted C-H activation arylation and decarboxylation.



**Scheme 2.2.** Decarboxylative C6 arylation using a bulky solvent

## 2.2. Experimental Section

### 2.2.1. General Information

All starting materials were commercially purchased and used without further purification. The reactions were conducted in Eyela™ process station (EPS) synthesiser tubes under ambient aerial conditions. TLC plates (Silica gel 60-F254 coated on aluminium plates from Merck) were visualised by either UV light or inside

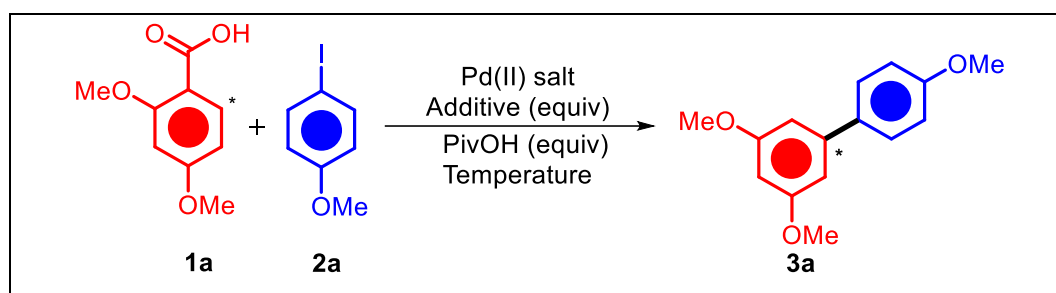
an iodine chamber.  $^1\text{H}$  and  $^{13}\text{C}$  NMR experiments were carried out using JEOL ECS-400MHz and Bruker Avance III 500 MHz and Bruker Avance III 600 MHz spectrometers, with chemical shifts referenced to tetramethyl silane (for  $^1\text{H}$ ) and  $\text{CDCl}_3$  (for  $^{13}\text{C}$  NMR) as internal standards. Purification of all products was achieved through column chromatography.

### 2.2.2. Optimisation of the reaction conditions

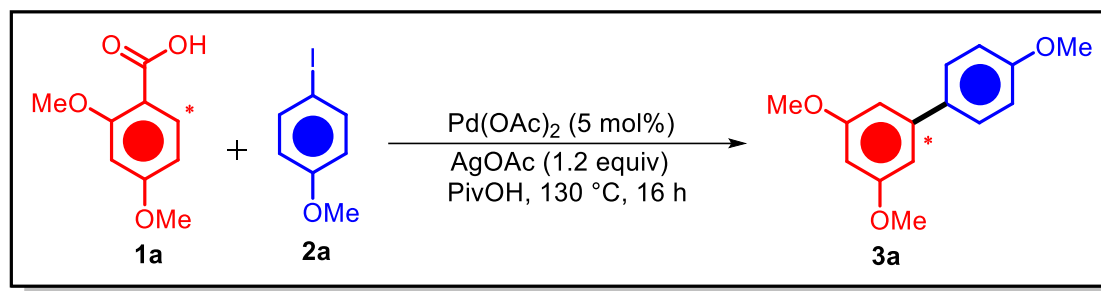
Our investigation began by selecting 2,4-dimethoxybenzoic acid (**1a**) and 4-iodoanisole (**2a**) as model substrates to determine optimal conditions. **Table 2.1** presents screening results under various conditions, including different palladium (II) salts, silver (I) salts, and parameters like temperature and reaction time (maintained at 130 °C for 16 hours) in pivalic acid. Initially, using 2 mol% of  $\text{Pd}(\text{OAc})_2$  and 1.2 equiv. of  $\text{Ag}_2\text{CO}_3$  resulted in a 41% yield of the *meta*-arylated product (**3a**) (**Table 2.1, Entry 1**). Replacing silver carbonate with silver acetate increased the yield to 49% (**Table 2.1, Entry 2**). Increasing  $\text{Pd}(\text{OAc})_2$  to 5 mol% while keeping other conditions constant further improved yields for both silver carbonate and silver acetate (**Table 2.1, Entries 3 and 4**).

Reducing pivalic acid to 3 equivalents yielded a 52% product yield with silver carbonate (**Table 2.1, Entry 5**), which increased to 61% with silver acetate (**Entry 6**) while maintaining pivalic acid at 3 equivalents. Reducing pivalic acid to 1.2 equivalents with other parameters unchanged resulted in a lower yield of 37% (**Entry 7**). Using 5 mol% of  $\text{Pd}(\text{TFA})_2$  did not improve yields with 6 or 3 equivalents of pivalic acid (**Entries 8 and 9**). Adding caesium acetate without silver acetate resulted in trace amounts of product (**Entry 10**), but with silver acetate, the yield was 34% (**Entry 11**), emphasizing the essential role of the silver salt. No product formed without a silver additive (**Entry 12**). Replacing silver acetate with silver trifluoroacetate decreased the yield (**Entry 13**). Other palladium catalysts like palladium (II) chloride yielded a 47% product (**Entry 14**). The reaction did not proceed at room temperature or 60 °C (**Entries 15 and 16**). The optimised conditions are summarised as follows: 2,4-dimethoxybenzoic acid (**1a**, 1 equivalent), 4-iodoanisole (**2a**, 1.2 equivalents),  $\text{Pd}(\text{OAc})_2$  (5 mol%),  $\text{AgOAc}$  (1.2 equivalents) in PivOH (3 equivalents) at 130 °C for 16 hours.

**Table 2.1.** Optimisation of the reaction conditions<sup>(a)</sup>

				
Sl. No.	Catalyst (mol%)	Additive (equiv.)	PivOH (equiv.)	Yield (%)
1	Pd(OAc) <sub>2</sub> (2)	Ag <sub>2</sub> CO <sub>3</sub> (1.2)	6	41%
2	Pd(OAc) <sub>2</sub> (2)	AgOAc (1.2)	6	49%
3	Pd(OAc) <sub>2</sub> (5)	Ag <sub>2</sub> CO <sub>3</sub> (1.2)	6	51%
4	Pd(OAc) <sub>2</sub> (5)	AgOAc (1.2)	6	58%
5	Pd(OAc) <sub>2</sub> (5)	Ag <sub>2</sub> CO <sub>3</sub> (1.2)	3	52%
6	<b>Pd(OAc)<sub>2</sub> (5)</b>	<b>AgOAc (1.2)</b>	<b>3</b>	<b>61%</b>
7	Pd(OAc) <sub>2</sub> (5)	AgOAc (1.2)	1.2	37%
8	Pd(TFA) <sub>2</sub> (5)	AgOAc (1.2)	6	32%
9	Pd(TFA) <sub>2</sub> (5)	AgOAc (1.2)	3	51%
10	Pd(OAc) <sub>2</sub> (5)	CsOAc (1.2)	3	Trace
11	Pd(OAc) <sub>2</sub> (5)	AgOAc (1.2), CsOAc (2)	3	34%
12	Pd(OAc) <sub>2</sub> (5)		3	NR
13	Pd(OAc) <sub>2</sub> (5)	AgTFA (1.2)	3	32%
14	PdCl <sub>2</sub> (5)	AgOAc (1.2)	3	47%
15	Pd(OAc) <sub>2</sub> (5)	AgOAc (1.2)	3	NR(a)
16	Pd(OAc) <sub>2</sub> (5)	AgOAc (1.2)	3	NR(b)
<sup>a</sup> <b>Reaction Conditions:</b> <b>1a</b> (1 equivalent, 0.3 mmol), <b>2a</b> (1.2 equivalents, 0.36 mmol), Temperature (130 °C), Time (16 hours).				

The optimised reaction can be shown as: 2,4-dimethoxybenzoic acid (**1a**, 1 equivalent), 4-iodoanisole (**2a**, 1.2 equivalents), Pd(OAc)<sub>2</sub> (5 mol%), AgOAc (1.2 equivalents) in PivOH (3 equivalents) at 130 °C for 16 hours (**Scheme 2.3**)



**Scheme 2.3.** Optimised reaction condition for C6-arylation

### 2.2.3. General procedure for C6 arylation of *ortho*-substituted benzoic acids.

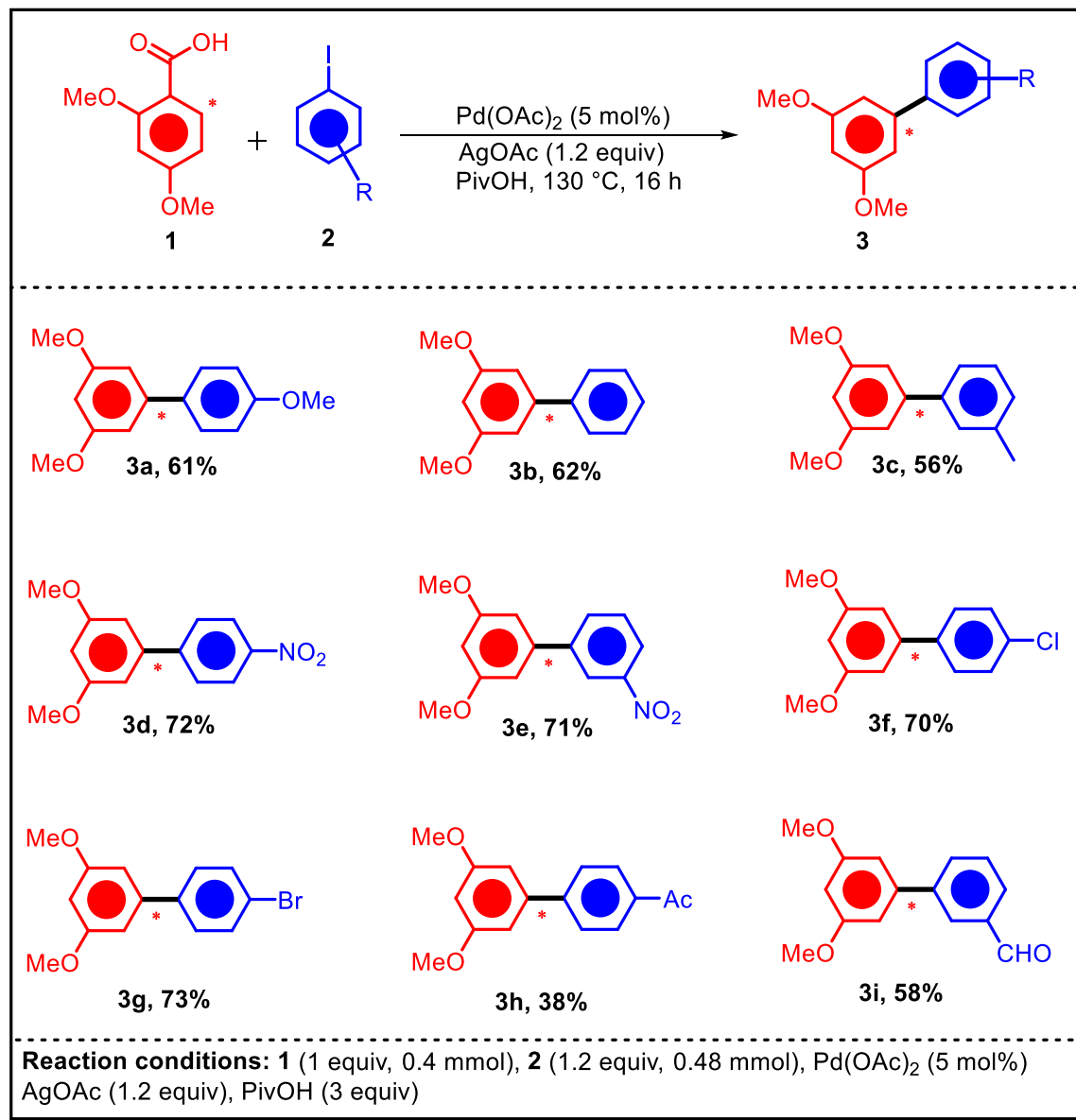
In a thoroughly cleaned and dried EPS synthesiser tube, 1 equivalent (0.5 mmol) of the *ortho*-substituted benzoic acid, 1.2 equivalents (0.6 mmol) of the iodoarene, 5 mol% (0.025 mmol) Palladium (II) acetate, 1.2 equivalents (0.6 mmol) of Silver (I) acetate, and 3 equivalents (1.5 mmol) of pivalic acid were added. The reaction was stirred at  $130\text{ }^\circ\text{C}$  for 16 hours and was monitored through TLC. After completion, the reaction mixture was treated with DCM and filtered through a plug of celite. The filtrate was washed with water and 5% potassium hydroxide solution, then extracted with DCM (3 x 10 mL). The combined organic layers were washed with brine and dried using anhydrous sodium sulfate. The crude product was purified using column chromatography (Hexanes) to yield the pure product.

### 2.2.4. Substrate Scope Studies

With the optimum conditions established, we explored the scope of the reaction using various substrates, while keeping the *ortho*-substituted carboxylic acid fixed (2,4-dimethoxybenzoic acid, **1a**) and varying the aryl iodide partner (**Table 2.2**). The electron-rich combination of 2,4-dimethoxybenzoic acid (**1a**) and 4-iodoanisole yielded a 61% yield (**3a**), and a similar yield of 62% (**3b**) was obtained by replacing 4-iodoanisole with iodobenzene. The yield dropped to 56% (**3c**) when the iodoarene was changed to 3-iodotoluene. Yields of the products increased with iodoarenes having electron-withdrawing substituents, reaching 72% (**3d**) with 4-iodonitrobenzene and 71% (**3e**) with 3-iodonitrobenzene. Di-halogenated substrates, 4-chloriodobenzene and 4-bromiodobenzene, provided yields of 70% (**3f**) and 73% (**3g**), respectively, with selectivity for iodides. Using 4-iodoacetophenone as the

coupling partner resulted in a 66% yield for product **3h**, which decreased to 58% (**3i**) when changing the aryl iodide to 3-iodobenzaldehyde.

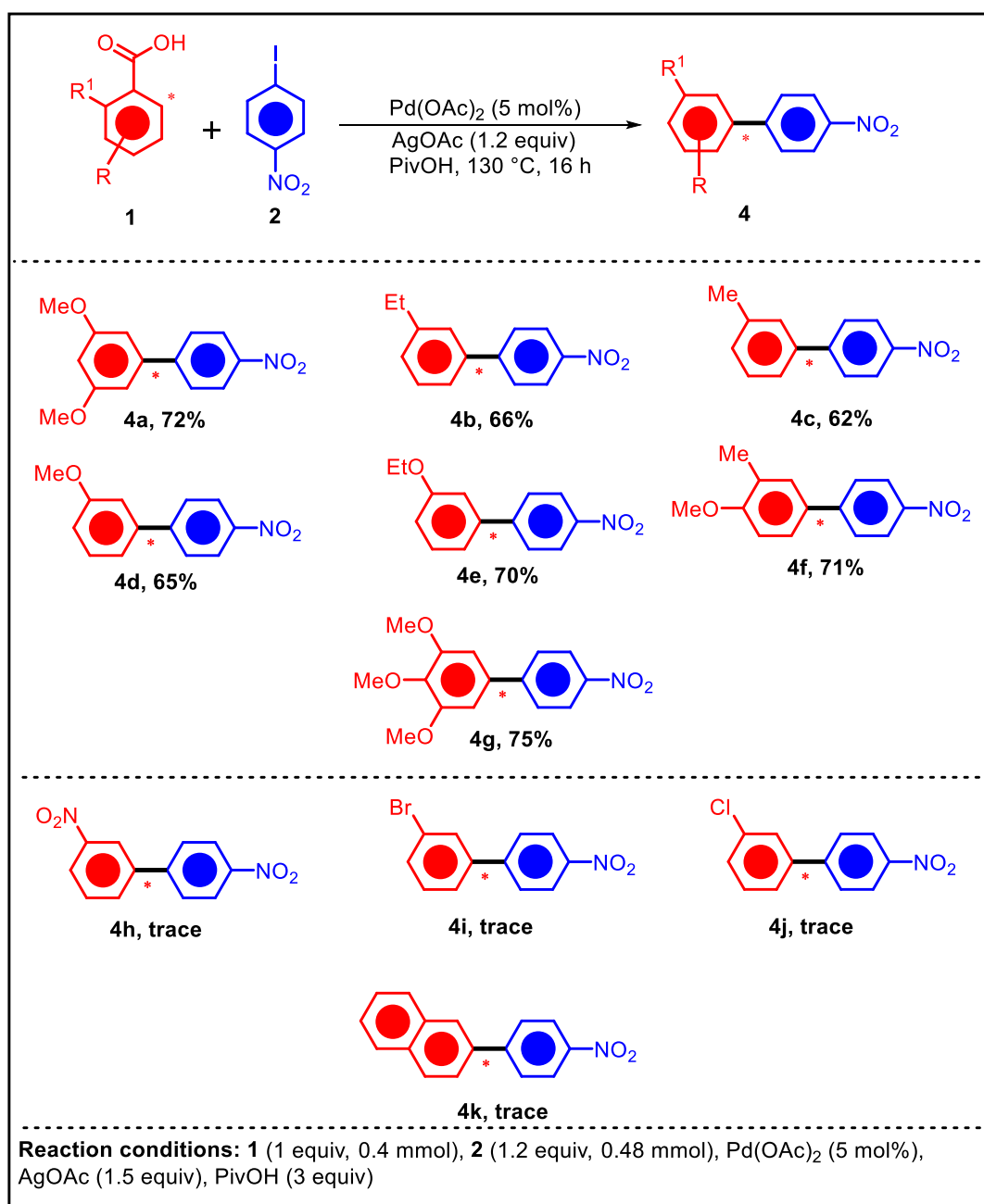
**Table 2.2.** Substrate scope with Iodoarenes



The reaction scope was further examined by keeping the iodoarene constant (4-iodonitrobenzene, **2d**) and varying the *ortho*-substituted carboxylic acid, as shown in **Table 2.3**. Initiating the reaction of **2d** with 2,4-dimethoxybenzoic acid (**1a**) yielded the product **4a** with a 72% yield. Changing the carboxylic acid to 2-ethyl benzoic acid resulted in a 66% yield (**4b**), which decreased to 62% with *o*-toluic acid (**4c**). Using *o*-anisic acid produced the product with a 65% yield (**4d**). A notable increase in product yield (**4e**) to 70% was observed when 2-ethoxybenzoic acid was employed with 4-

iodonitrobenzene. Similarly, yields of 71% and 75% were achieved with electron-rich 2-methyl-3-methoxybenzoic acid and 2,3,4-trimethoxybenzoic acid, respectively (**4f** and **4g**). Unfortunately, substrates with *ortho*-electron-withdrawing substituents, such as 2-nitrobenzoic acid (**1h**, **4h**), and 2-bromobenzoic acid (**1i**, **4i**), failed to yield satisfactory amounts of arylated products, obtaining only trace amounts. 2-Chlorobenzoic acid (**1j**, **4j**) showed no conversion, and  $\alpha$ -naphthoic acid (**1k**, **4k**) did not display any reaction at all.

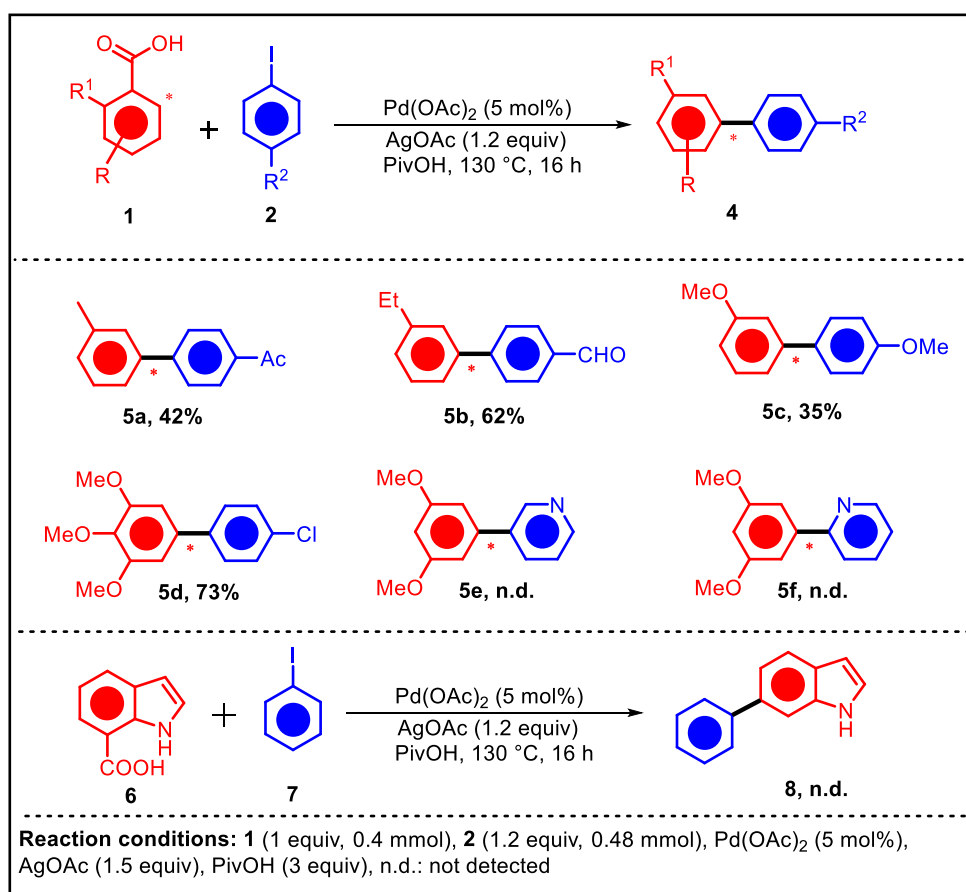
**Table 2.3.** Substrate scope with benzoic acids





The results presented in **Table 2.2** and **Table 2.3**, indicate that the reaction performs more favourably when the carboxylic acid partner features electron-donating groups, while the iodoarene incorporates electron-withdrawing groups. To study this, specific substrates were selected, and reactions were conducted as summarised in **Table 2.4**. It was observed that a decrease in the number of electron-pulling groups on the benzene ring of the carboxylic acid resulted in a lower yield. **Entries 5a** and **5b** in **Table 2.4** demonstrate that an increase in the electron-withdrawing power of the group on the benzene ring of the iodoarene directed a rise in the yield, 42% and 62% respectively. Additionally, the presence of electron-pushing groups (+R effect) on both the carboxylic acid and the iodoarene contributed to a decrease in product yield to 35% (**5c**). An increase in number of electron-pushing groups led to a increase in yield to 73% in the existence of the electron-withdrawing chloride group in the iodoarene segment (**5d**). The reaction was not seen to yield the desired products upon using 2-iodopyridine, 3-iodopyridine (**5e** and **5f**) and with indole-7-carboxylic acid (**8**).

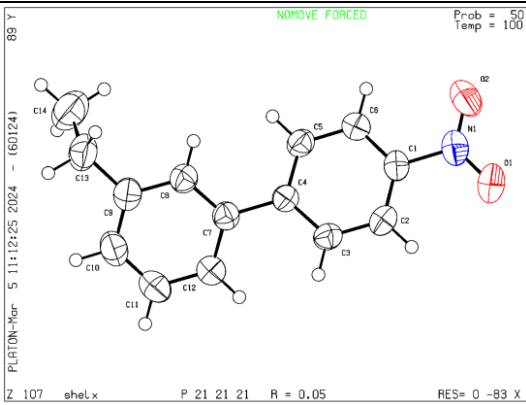
**Table 2.4.** Scope with *o*-toluic, *o*-anisic and 2,3,4-trimethoxybenzoic acids



### 2.2.5. X Ray Crystallography

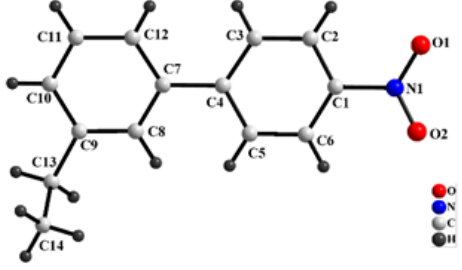
A single crystal of **3bd**, suitable for diffraction measurement, was directly used from the reaction mixtures. Diffraction data for the compound were collected on a Bruker APEX-II CCD Diffractometer using MoK $\alpha$  radiation ( $\lambda=0.71073$  Å) with  $\varphi$  and  $\omega$  scans of narrow ( $0.5^\circ$ ) frames at 100 K. The structure was solved using direct methods with SHELXL-97 as implemented in the WinGX [29] program system. Anisotropic refinement was performed on all non-hydrogen atoms. Aliphatic and aromatic hydrogen atoms were placed at calculated positions but allowed on their parent atoms during subsequent refinement cycles (**Table 2.5**). Some of the selected bond lengths and angles are represented in **Table 2.6**.

**Table 2.5.** Molecular structure (ORTEP Diagram) of **3bd** with 50% probability ellipsoids along with crystallographic data.

	
Empirical formula	C <sub>14</sub> H <sub>13</sub> N <sub>1</sub> O <sub>2</sub>
Formula weight	227.25
Temperature/K	100 (2)
Wavelength	0.71073 Å
CCDC	2280001
Crystal system	Orthorhombic
Space group	P2 <sub>1</sub> 2 <sub>1</sub> 2 <sub>1</sub>
a/Å	7.383(3)
b/Å	12.408(5)
c/Å	12.784(5)
$\alpha/^\circ$	90

$\beta/^\circ$	90
$\gamma/^\circ$	90
Volume [ $\text{\AA}^3$ ]	1171.1(8)
Z	4
$\rho_{\text{calc}}$ [ $\text{Mg}/\text{m}^3$ ]	1.289
$\mu$ [ $\text{mm}^{-1}$ ]	0.087
F(000)	480
Crystal size [ $\text{mm}^3$ ]	0.18 x 0.14 x 0.12
Theta range for data collection	2.287° to 28.416°
Index ranges	-9 $\leq h \leq$ 9, -16 $\leq k \leq$ 16, -17 $\leq l \leq$ 17
Reflections collected	47843
Independent reflections	2937 [R(int) = 0.0726]
Completeness to theta = 25.242°	100.0 %
Refinement method	Full-matrix least-squares on $F^2$
Data / restraints / parameters	2937/0/156
Goodness-of-fit on $F^2$	0.927
Final R indices [ $I > 2\sigma(I)$ ]	R1 = 0.0474, wR2 = 0.1224
R indices (all data)	R1 = 0.0788, wR2 = 0.1479

**Table 2.6.** Selected bond lengths and bond angles of **4b**.

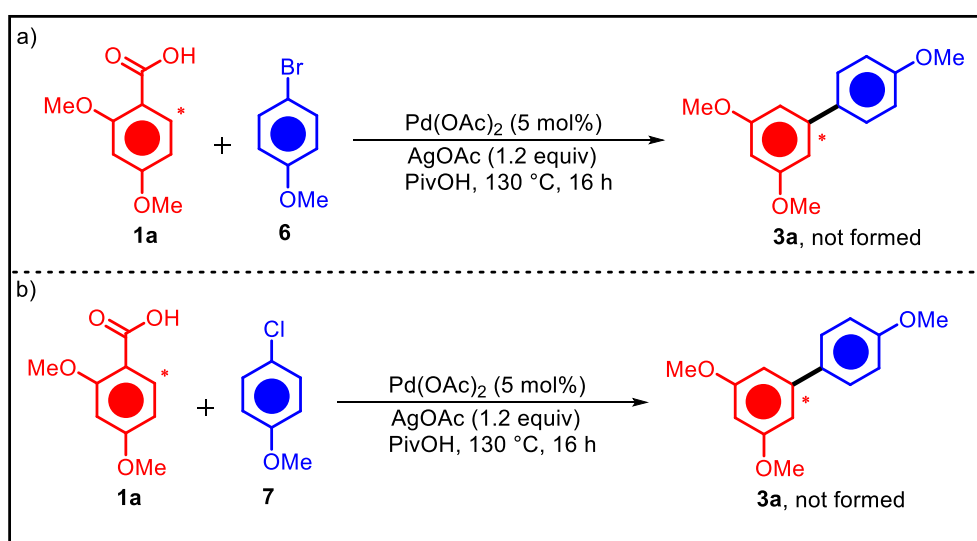
			
Bond Length [ $\text{\AA}$ ]			
O(1)-N(1)	1.223(3)	C(7)-C(8)	1.389(3)
O(2)-N(1)	1.219(3)	C(7)-C(12)	1.391(4)
N(1)-C(1)	1.462(3)	C(8)-C(9)	1.395(3)
C(1)-C(2)	1.377(4)	C(9)-C(10)	1.380(4)
C(1)-C(6)	1.380(4)	C(9)-C(13)	1.507(4)

C(2)-C(3)	1.374(4)	C(10)-C(11)	1.381(4)
C(4)-C(5)	1.396(3)	C(11)-C(12)	1.392(4)
C(4)-C(7)	1.480(3)	C(13)-C(14)	1.488(5)
C(5)-C(6)	1.380(4)		
Bond angles [°]			
O(2)-N(1)-O(1)	122.6(2)	C(3)-C(2)-C(1)	121.5(2)
O(2)-N(1)-C(1)	118.7(3)	C(2)-C(3)-C(4)	121.5(2)
O(1)-N(1)-C(1)	118.7(2)	C(5)-C(4)-C(3)	118.0(2)
C(2)-C(1)-C(6)	119.5(2)	C(5)-C(4)-C(7)	121.1(2)
C(2)-C(1)-N(1)	118.7(2)	C(3)-C(4)-C(7)	121.0(2)
C(6)-C(1)-N(1)	118.8(2)	C(6)-C(5)-C(4)	121.2(2)

### 2.2.6. Control Experiments

#### 2.2.6.1. Reaction with aryl chlorides and bromides

When the reaction was conducted **1a** and 4-bromoanisole (**Scheme 2.4(a)**) and 4-chloroanisole (**Scheme 2.4(b)**) under the specified conditions, no formation of the desired product was observed, and the starting carboxylic acid was recovered. This observation further confirms the formation of product **3a** (**Table 2.2**) through selective cleavage of the C-I bond.



**Scheme 2.4.** Reaction of **1a** with 4-bromoanisole (**6**) and 4-chloroanisole (**7**)

### 2.2.6.2. Protodecarboxylation experiments

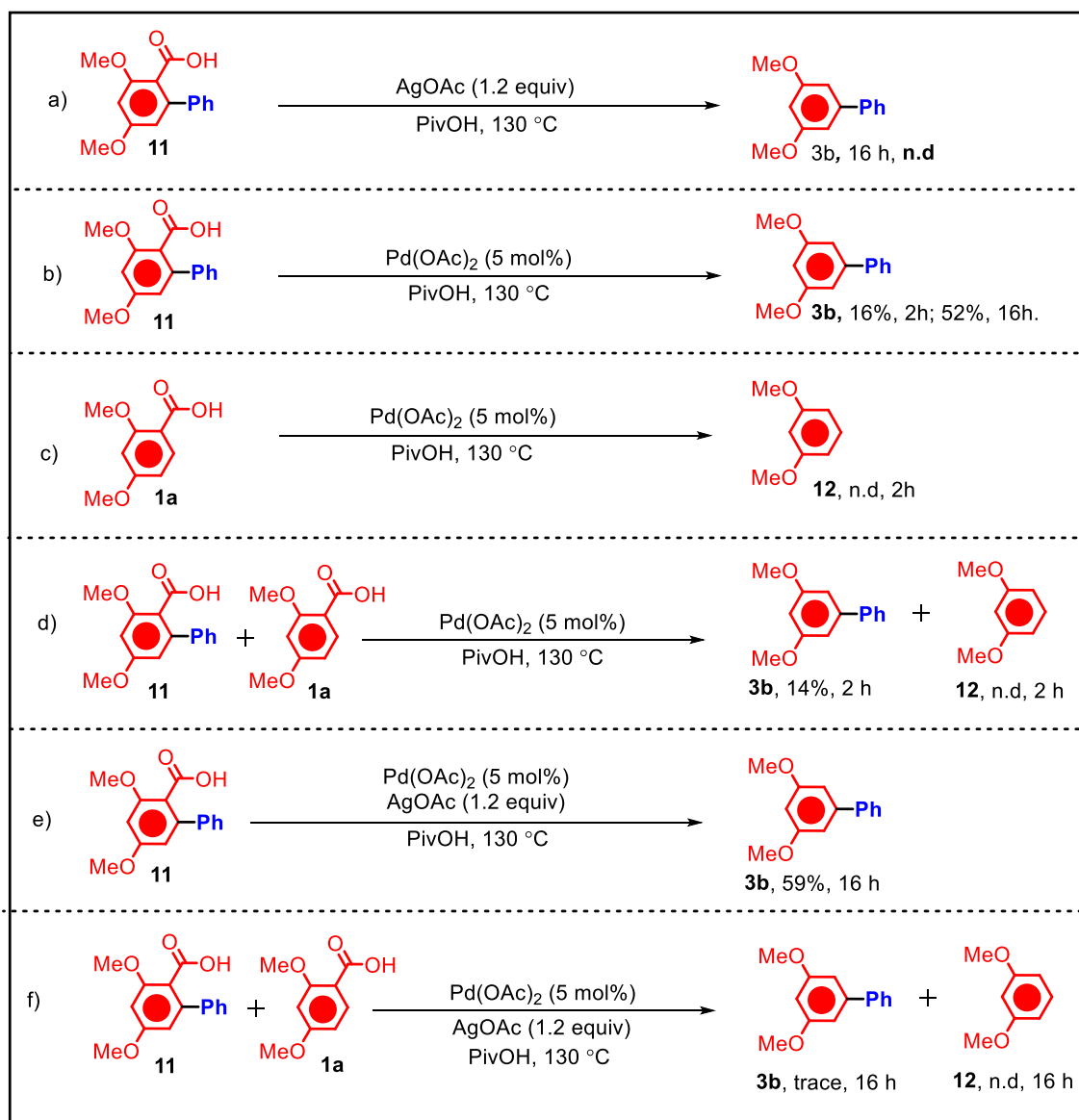
Furthermore, compared to the non-arylated carboxylic acid (**1a**), the C6-arylated carboxylic acid [25], has proven to be superior towards protodecarboxylation which in turn shows the reaction to follow a C6 arylation-protodecarboxylation cascade pathway under the given conditions, like the condition reported by Larrosa and co-workers [21]. Initially, it was investigated whether silver played a role in the decarboxylation step under the given conditions. It was seen that in the absence of Pd, no decarboxylation of the *ortho*-arylated substrate occurred. It was observed that in the absence of Pd, no decarboxylation of the *ortho*-arylated substrate occurred. Subsequently, the Pd(II)–PivOH system was employed for the decarboxylation of both the *ortho*-arylated substrate and the carboxylic acid "**1a**" separately. The results were consistent with previous reports indicating that Pd(II)-catalysed decarboxylation reactions favor sterically hindered carboxylic acids [20]. The *ortho*-arylated substrate underwent decarboxylation, yielding 16% of the product in 2 hours, which increased to 49% in 12 hours. However, **1a** did not undergo decarboxylation even after 16 hours. Similarly, when a 1:1 mixture of the *ortho*-arylated substrate and **1a** was tested, the product **3ab** was isolated with a 14% yield in 2 hours, with **1a** remaining completely unreacted. Furthermore, under optimised reaction conditions, the decarboxylation of the *ortho*-arylated substrate yielded 59% of the product in 16 hours. To study the competitive decarboxylation of the *ortho*-arylated substrate and **1a**, a 1:1 mixture of both was subjected to decarboxylation under optimised conditions, yielding trace amounts of product **3ab** in 16 hours. This could be due to the rapid formation of a palladacycle with the silver salt of **1a**, rendering the route ineffective. All these results have been summarised in **Scheme 2.5**.

### 2.2.7. Plausible Reaction Mechanism

Based on the observations made in the protodecarboxylation step and the previous literature reports, the following plausible reaction mechanism can be given.

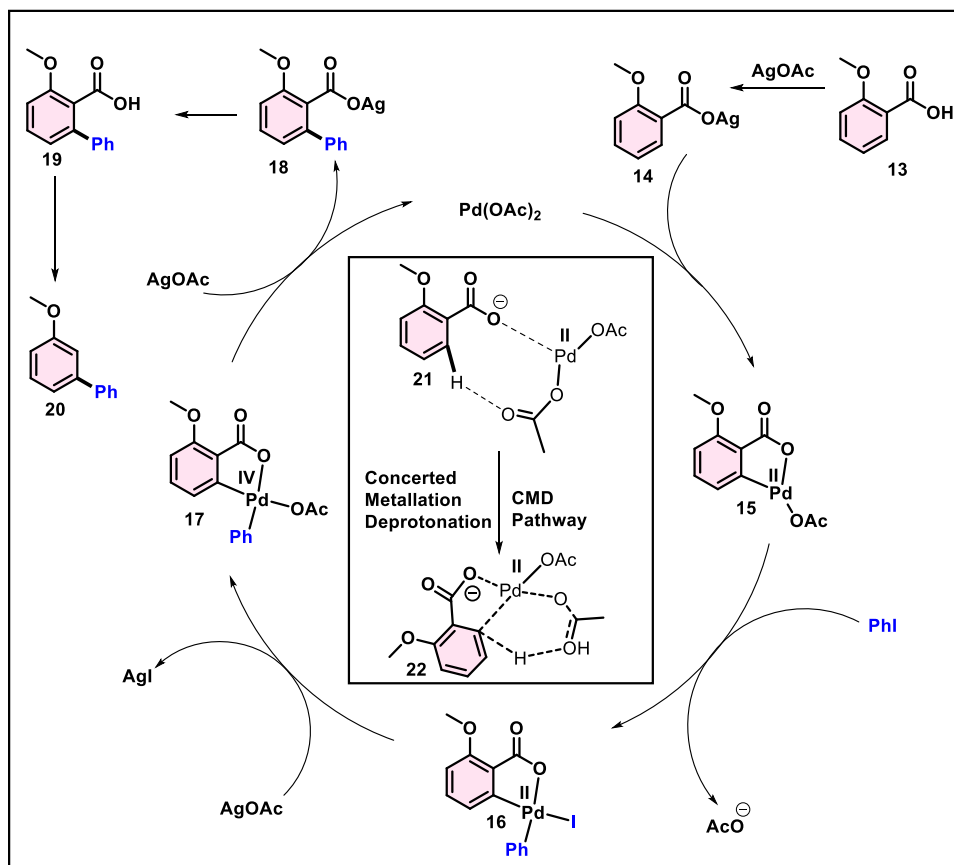
The reaction proceeds through a sequence of discrete steps. Initially, an oxidative addition event takes place, wherein the aryl iodide reacts with the Pd(0) center, resulting in the formation of the aryl palladium (II) iodide. This intermediate subsequently undergoes iodide exchange with silver benzoate, a product derived

from the reaction between benzoic acid and silver acetate, leading to the generation of a distinct chemical species denoted as (3). In a pivotal kinetic step (r.d.s.), (3) undergoes cyclisation to form a 5-membered palladacycle. The subsequent reductive elimination, facilitated by Ag (I), yields the C6 aryl silver salt of carboxylic acid (6). Upon protonation, (6) undergoes transformation into the species denoted as (7). The final stage entails protodecarboxylation assisted by Pd(II), culminating in the desired product formation (13). This has been verified through computational studies (Scheme 2.6). This has been verified through computational studies.

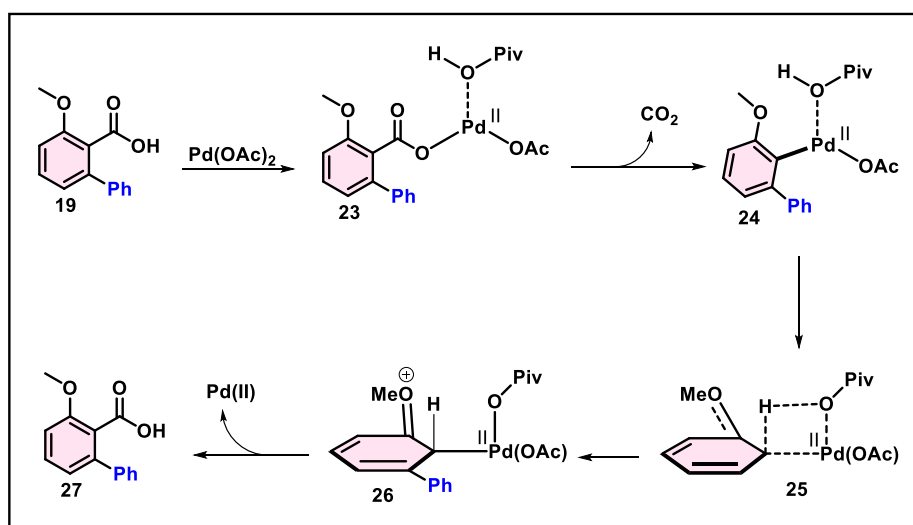


**Scheme 2.5.** Protodecarboxylation experiments with the *ortho*-arylated carboxylic acid

Dickstein *et al.* have already studied the pathway of Pd(II)-catalysed protodecarboxylation of *o,o'*-disubstituted benzoic acids (**Scheme 2.7**). This step follows a concerted proton transfer pathway succeeding carboxyl palladation and decarboxylation.



**Scheme 2.6.** Mechanistic pathway of the C6 arylation step



**Scheme 2.7.** Concerted proton transfer mechanism for protodecarboxylation

### 2.2.8. Computational studies

#### 2.2.8.1. Computational details

All the structures were fully optimised at M06-2X/def2-TZVP 1 [27] level in gas phase at 298K and 1 atm pressure (**Figure 2.1**). Harmonic vibrational frequency calculations were performed at the same level to understand the nature of the stationary points. All structures were found to be true minimum except the transition state which contains one imaginary mode of vibration. All energies are zero point and thermal corrected. All these calculations were performed using Gaussian 16 suite of program [28].

**Figure 2.1** shows the energetics for the proposed mechanism. The rate determining step involving C-H activation *via* concerted metalation deprotonation (CMD) pathway involves a barrier of only 12.4 kcal/mol including zero-point correction. In the transition state the O...H and C...H distances are 1.431 and 1.670 Å respectively. Other steps are exergonic ( $\Delta$  (PPM)G < 0) in nature except the last step which is endergonic in nature by 17.8 kcal/mol. The last step involves regeneration of Pd(OAc)<sub>2</sub> along with the silver complex of CH<sub>3</sub>OC<sub>6</sub>H<sub>4</sub>Ph. Overall, the steps are exergonic which implies that the CMD pathway for C-H activation is energetically favourable. **Table 2.7** shows the stepwise Gibbs energy changes.

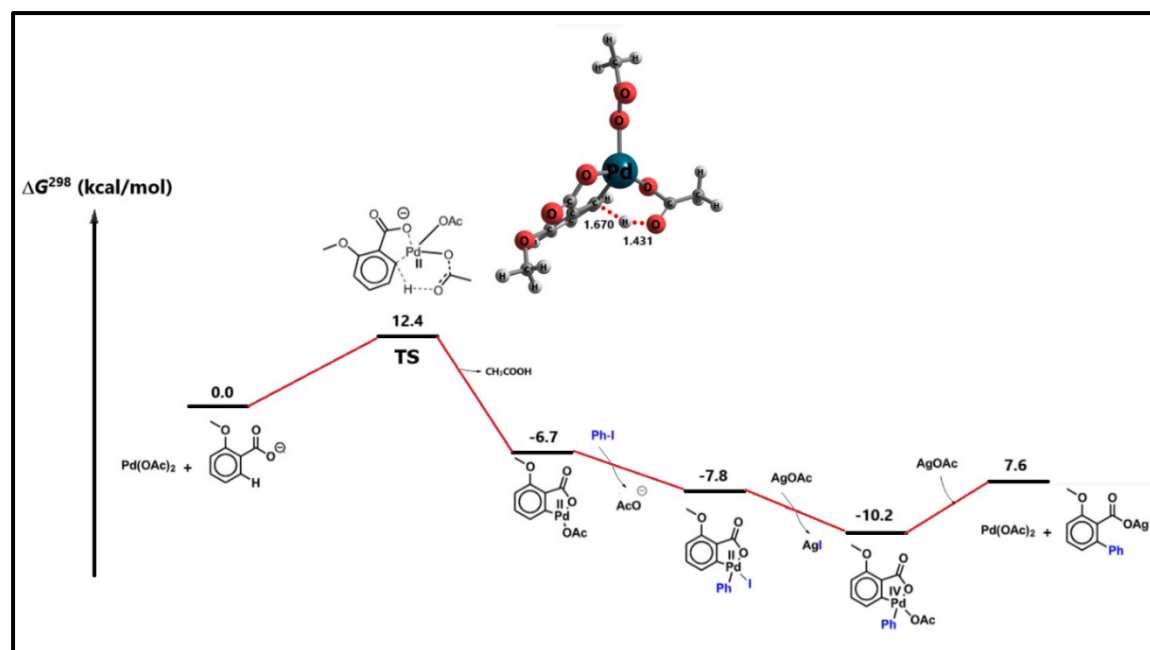


**Figure 2.1.** Proposed reaction's potential energy diagram calculated using the M06-2X/def2-TZVP 1 level of theory



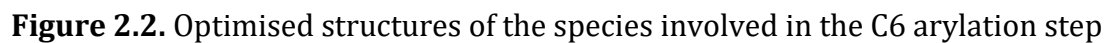
All the reaction species and transition states implicated in the proposed plausible reaction path have been examined on the potential energy surface (PES), as illustrated in **Figure 2.1**. **Table 2.7** shows the corresponding stepwise Gibbs energy changes.

**Table 2.7.** Stepwise Gibbs' free energy changes.

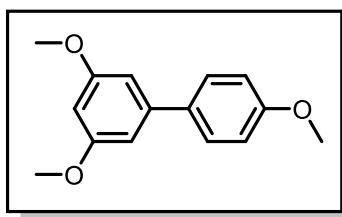
Step	$\Delta G$ (kcal/mol)
1	12.4
2	-19.1
3	-1.1
4	-2.4
5	17.8

### 2.2.8.2. Electronic Structures

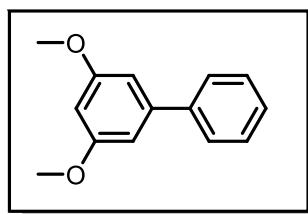
**Figure 2.2** represents the optimised structures of the species involved in the C6 arylation step



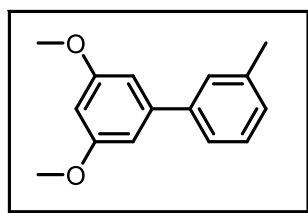
In summary, we have developed a protocol for Pd(II)-catalysed C1 decarboxylative C6 arylation of *ortho*-substituted benzoic acids using pivalic acid medium. This procedure results in the formation of *meta*-arylated biphenyls, employing a traceless C-H activation directing group strategy. Notably, the reaction follows an *ortho*-arylation-decarboxylation pathway, with the Pd(II) center facilitating the decarboxylation step. Computational studies provide additional insights into the tandem pathway employed by the reaction.

2.4  $^1\text{H}$  and  $^{13}\text{C}$  NMR Data

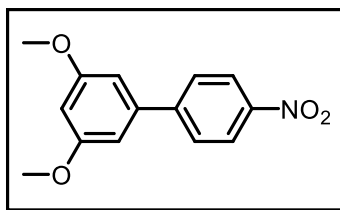
**3a. 3,4',5-Trimethoxy-1,1'-biphenyl**, white solid:  $^1\text{H}$  NMR (400 MHz,  $\text{CHCl}_3$ - $d_3$ )  $\delta$  (ppm) 7.50 (d,  $J = 8.6$  Hz, 2H), 6.95 (d,  $J = 8.6$  Hz, 2H), 6.68 (d,  $J = 2.0$  Hz, 2H), 6.42 (t,  $J = 2.2$  Hz, 1H), 3.84 (s, 3H), 3.83 (s, 6H).  $^{13}\text{C}$  NMR (100 MHz,  $\text{CHCl}_3$ - $d_3$ )  $\delta$  (ppm) 161.1, 159.4, 143.2, 133.8, 128.3, 114.2, 105.2, 98.8, 55.5, 55.4.



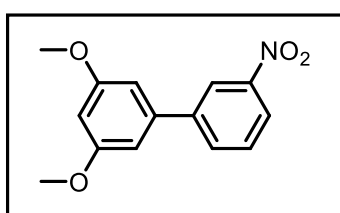
**3b. 3,5-Dimethoxy-1,1'-biphenyl**, colourless oil:  $^1\text{H}$  NMR (400 MHz,  $\text{CHCl}_3$ - $d_3$ )  $\delta$  (ppm) 7.57 (dd,  $J = 8.3, 1.3$  Hz, 2H), 7.45 – 7.40 (m, 2H), 7.37 – 7.32 (m, 1H), 6.73 (d,  $J = 2.3$  Hz, 2H), 6.47 (t,  $J = 2.3$  Hz, 1H), 3.84 (s, 6H).  $^{13}\text{C}$  NMR (100 MHz,  $\text{CHCl}_3$ - $d_3$ )  $\delta$  (ppm) 161.1, 143.6, 141.3, 128.8, 127.5, 105.5, 99.4, 55.7, 46.5.



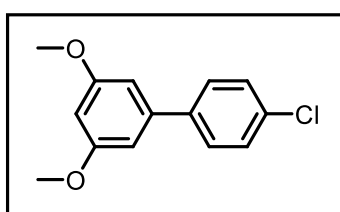
**3c. 3,5-Dimethoxy-3'-methyl-1,1'-biphenyl**, colourless oil:  $^1\text{H}$  NMR (400 MHz,  $\text{CHCl}_3$ - $d_3$ )  $\delta$  (ppm) 7.40 – 7.35 (m, 2H), 7.34 – 7.28 (m, 1H), 7.19 – 7.14 (m, 1H), 6.72 (d,  $J = 2.3$  Hz, 2H), 6.46 (t,  $J = 2.3$  Hz, 1H), 3.84 (s, 6H), 2.41 (s, 3H).  $^{13}\text{C}$  NMR (100 MHz,  $\text{CHCl}_3$ - $d_3$ )  $\delta$  (ppm) 161.2, 143.7, 41.3, 138.4, 128.7, 128.4, 128.1, 124.4, 105.5, 99.3, 55.5, 21.6.



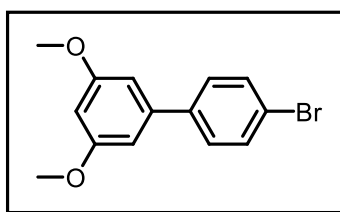
**3d. 3,5-Dimethoxy-4'-nitro-1,1'-biphenyl**, white solid:  $^1\text{H}$  NMR (400 MHz, CHLOROFORM-D)  $\delta$  (ppm) 8.27 (d,  $J$  = 8.9 Hz, 2H), 7.70 (d,  $J$  = 8.9 Hz, 2H), 6.72 (d,  $J$  = 2.2 Hz, 2H), 6.53 (t,  $J$  = 2.2 Hz, 1H), 3.85 (s, 6H).  $^{13}\text{C}$  NMR (100 MHz, CHLOROFORM-D)  $\delta$  (ppm) 161.4, 147.7, 141.0, 128.0, 124.1, 105.8, 102.4, 100.6, 55.6.



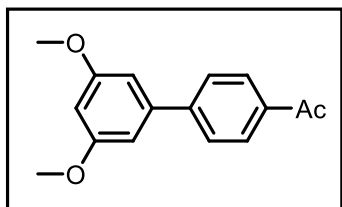
**3e. 3,5-Dimethoxy-3'-nitro-1,1'-biphenyl**, white solid:  $^1\text{H}$  NMR (400 MHz, CHLOROFORM-D)  $\delta$  (ppm) 8.42 (t,  $J$  = 2.0 Hz, 1H), 8.19 (dd,  $J$  = 7.9, 2.5 Hz, 1H), 7.88 (dd,  $J$  = 7.8, 1.1 Hz, 1H), 7.58 (t,  $J$  = 8.0 Hz, 1H), 6.72 (d,  $J$  = 2.2 Hz, 2H), 6.52 (t,  $J$  = 2.2 Hz, 1H), 3.85 (s, 6H).  $^{13}\text{C}$  NMR (100 MHz, CHLOROFORM-D)  $\delta$  (ppm) 161.4, 148.7, 142.9, 140.9, 133.2, 129.8, 129.7, 122.2, 105.6, 100.4, 55.7.



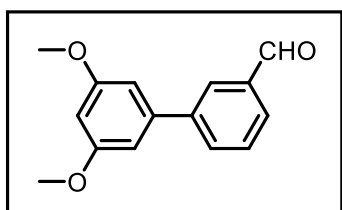
**3f. 4'-Chloro-3,5-dimethoxy-1,1'-biphenyl**, white solid:  $^1\text{H}$  NMR (400 MHz, CHLOROFORM-D)  $\delta$  (ppm) 7.49 (d,  $J$  = 8.6 Hz, 2H), 7.38 (d,  $J$  = 8.6 Hz, 2H), 6.67 (d,  $J$  = 2.2 Hz, 2H), 6.46 (t,  $J$  = 2.2 Hz, 1H), 3.83 (s, 6H).  $^{13}\text{C}$  NMR (100 MHz, CHLOROFORM-D)  $\delta$  (ppm) 161.2, 142.3, 139.7, 133.7, 128.9, 128.5, 105.4, 99.5, 55.6.



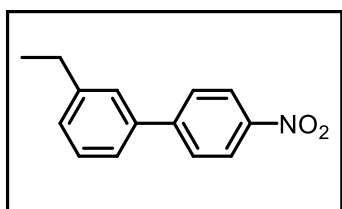
**3g. 4'-Bromo-3,5-dimethoxy-1,1'-biphenyl, white solid:**  $^1\text{H}$  NMR (400 MHz, CHLOROFORM-D)  $\delta$  (ppm) 7.54 (d,  $J$  = 8.4 Hz, 2H), 7.42 (d,  $J$  = 8.5 Hz, 2H), 6.67 (d,  $J$  = 2.2 Hz, 2H), 6.47 (t,  $J$  = 2.2 Hz, 1H), 3.83 (s, 6H).  $^{13}\text{C}$  NMR (100 MHz, CHLOROFORM-D)  $\delta$  (ppm) 161.2, 142.3, 140.2, 131.9, 128.9, 121.9, 105.4, 99.5, 55.6.



**3h. 1-(3',5'-Dimethoxy-[1,1'-biphenyl]-4-yl)ethan-1-one, colourless oil:**  $^1\text{H}$  NMR (400 MHz, CHLOROFORM-D)  $\delta$  (ppm) 8.00 (d,  $J$  = 8.5 Hz, 2H), 7.65 (d,  $J$  = 8.5 Hz, 2H), 6.74 (d,  $J$  = 2.2 Hz, 2H), 6.50 (t,  $J$  = 2.2 Hz, 1H), 3.84 (s, 6H), 2.62 (s, 3H),  $^{13}\text{C}$  NMR (100 MHz, CHLOROFORM-D)  $\delta$  (ppm) 197.9, 161.3, 145.8, 142.2, 136.2, 128.9, 127.4, 105.7, 100.1, 55.6, 26.8.

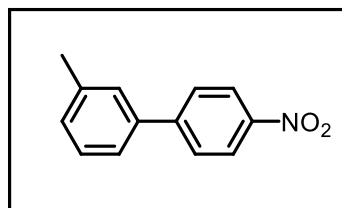


**3i. 3',5'-Dimethoxy-[1,1'-biphenyl]-3-carbaldehyde, white solid:**  $^1\text{H}$  NMR (500 MHz, CHLOROFORM-D)  $\delta$  (ppm) 10.08 (s, 1H), 8.08 (s, 1H), 7.89 – 7.80 (m, 2H), 7.60 (t,  $J$  = 7.7 Hz, 1H), 6.75 (d,  $J$  = 2.2 Hz, 2H), 6.51 (t,  $J$  = 2.2 Hz, 1H), 3.86 (s, 6H).  $^{13}\text{C}$  NMR (125 MHz, CHLOROFORM-D)  $\delta$  (ppm) 192.2, 161.2, 142.2, 141.9, 136.9, 133.1, 129.4, 128.9, 128.2, 105.5, 99.95, 55.5.

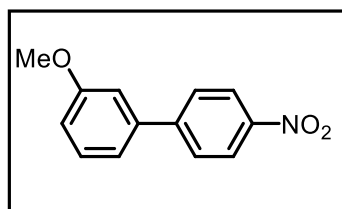


**4b. 3-Ethyl-4'-nitro-1,1'-biphenyl, White Solid:**  $^1\text{H}$  NMR (600 MHz, CHLOROFORM-D)  $\delta$  (ppm) 8.32 (d,  $J$  = 8.8 Hz, 2H), 7.76 (d,  $J$  = 8.8 Hz, 2H), 7.49 – 7.41 (m, 3H), 7.32 (d,  $J$  = 7.2 Hz, 1H), 2.77 (q,  $J$  = 7.6 Hz, 2H), 1.33 (t,  $J$  = 7.6 Hz, 3H).  $^{13}\text{C}$  NMR (150 MHz,

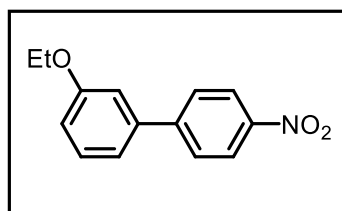
CHLOROFORM-D)  $\delta$  (CHLOROFORM-D) 147.9, 147.0, 145.3, 138.8, 129.1, 128.5, 127.8, 127.0, 124.8, 124.1, 28.9, 15.6.



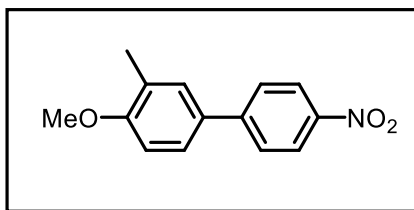
**4c. 3-Methyl-4'-nitro-1,1'-biphenyl**, yellow solid:  $^1\text{H}$  NMR (400 MHz, CHLOROFORM-D)  $\delta$  (ppm) 8.28 (d,  $J$  = 8.9 Hz, 2H), 7.72 (d,  $J$  = 8.9 Hz, 2H), 7.39 (m, 3H), 7.28 – 7.17 (m, 1H), 2.43 (s, 3H).  $^{13}\text{C}$  NMR (100 MHz, CHLOROFORM-D)  $\delta$  (ppm) 147.9, 147.1, 139.0, 138.8, 129.8, 129.2, 128.3, 127.9, 124.6, 124.2, 21.6.



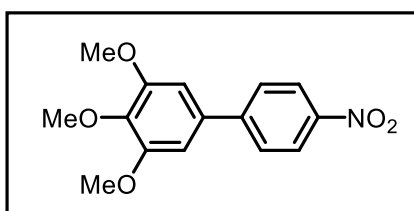
**4d. 3-Methoxy-4'-nitro-1,1'-biphenyl**, pale yellow solid:  $^1\text{H}$  NMR (600 MHz, CHLOROFORM-D)  $\delta$  (ppm) 8.31 (d,  $J$  = 8.8 Hz, 2H), 7.75 (d,  $J$  = 8.8 Hz, 2H), 7.44 (t,  $J$  = 8.0 Hz, 1H), 7.23 (d,  $J$  = 7.7 Hz, 1H), 7.18 – 7.15 (m, 1H), 7.01 (dd,  $J$  = 8.2, 2.1 Hz, 1H), 3.91 (s, 3H).  $^{13}\text{C}$  NMR (150 MHz, CHLOROFORM-D)  $\delta$  (ppm) 160.2, 147.5, 147.2, 140.3, 130.2, 127.9, 124.1, 119.8, 114.1, 113.3, 55.4.



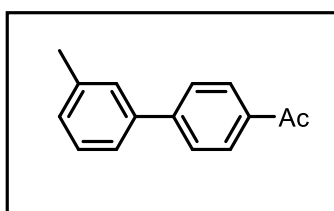
**4e. 3-Ethoxy-4'-nitro-1,1'-biphenyl**, pale yellow solid:  $^1\text{H}$  NMR (500 MHz,  $\text{CDCl}_3$ )  $\delta$  (ppm) 8.29 (d,  $J$  = 8.8 Hz, 2H), 7.72 (d,  $J$  = 8.8 Hz, 2H), 7.39 (t,  $J$  = 7.9 Hz, 1H), 7.19 (d,  $J$  = 7.7 Hz, 1H), 7.16 – 7.11 (m, 1H), 6.97 (dd,  $J$  = 8.2, 2.1 Hz, 1H), 4.11 (q,  $J$  = 7.0 Hz, 2H), 1.46 (t,  $J$  = 7.0 Hz, 3H).  $^{13}\text{C}$  NMR (126 MHz,  $\text{CDCl}_3$ )  $\delta$  (ppm) 159.6, 147.6, 147.2, 140.2, 130.2, 127.8, 124.1, 119.7, 114.7, 113.9, 63.7, 14.8.



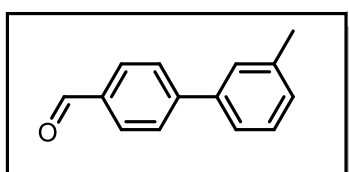
**4f, 4-Methoxy-3-methyl-4'-nitro-1,1'-biphenyl**, yellow solid:  $^1\text{H}$  NMR (600 MHz, CHLOROFORM-D)  $\delta$  (ppm) 8.29 (d,  $J$  = 8.5 Hz, 2H), 7.72 (d,  $J$  = 8.5 Hz, 2H), 7.55 – 7.38 (m, 2H), 6.96 (d,  $J$  = 8.4 Hz, 1H), 3.92 (s, 3H), 2.33 (s, 3H).  $^{13}\text{C}$  NMR (150 MHz, CHLOROFORM-D)  $\delta$  (ppm) 158.7, 147.4, 146.4, 130.6, 129.6, 127.6, 127.0, 125.0, 124.1, 110.4, 55.5, 16.4.



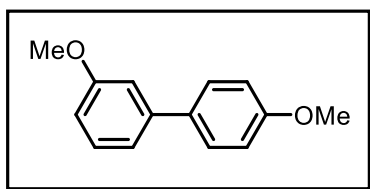
**4g, 3,4,5-Trimethoxy-4'-nitro-1,1'-biphenyl**, pale yellow solid:  $^1\text{H}$  NMR (600 MHz, CHLOROFORM-D)  $\delta$  (ppm) 8.31 (d,  $J$  = 8.8 Hz, 2H), 7.72 (d,  $J$  = 8.8 Hz, 2H), 6.82 (s, 2H), 3.97 (s, 6H), 3.94 (s, 3H).  $^{13}\text{C}$  NMR (150 MHz, CHLOROFORM-D)  $\delta$  (ppm) 153.8, 147.7, 147.0, 139.0, 134.6, 127.7, 124.1, 104.8, 61.0, 56.3.



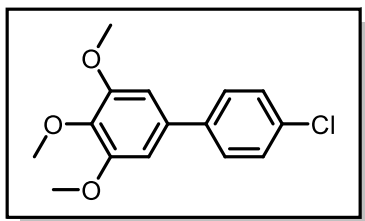
**5a, 1-(3'-Methyl-[1,1'-biphenyl]-4-yl)ethan-1-one**, white solid:  $^1\text{H}$  NMR (400 MHz, CHLOROFORM-D)  $\delta$  (ppm) 8.02 (d,  $J$  = 8.6 Hz, 2H), 7.67 (d,  $J$  = 8.6 Hz, 2H), 7.43 (m, 2H), 7.41 (m, 1H), 7.35 (m, 1H), 2.63 (s, 3H), 2.43 (s, 3H).  $^{13}\text{C}$  NMR (100 MHz, CHLOROFORM-D)  $\delta$  (ppm) 198.0, 146.0, 139.9, 138.7, 135.8, 129.1, 129.0, 128.9, 128.1, 127.3, 124.5, 26.8, 21.6.



**5b. 3'-Methyl-[1,1'-biphenyl]-4-carbaldehyde**, colourless liquid:  $^1\text{H}$  NMR (600 MHz, CHLOROFORM-D)  $\delta$  (ppm) 10.08 (s, 1H), 7.97 (d,  $J = 8.2$  Hz, 2H), 7.77 (d,  $J = 8.2$  Hz, 2H), 7.47 (m, 2H), 7.40 (m, 1H), 7.27 (m, 1H), 2.47 (s, 3H).  $^{13}\text{C}$  NMR (150 MHz, CHLOROFORM-D)  $\delta$  (ppm) 192.0, 147.4, 139.7, 138.7, 135.1, 130.3, 129.3, 128.9, 128.1, 127.7, 124.5, 21.5.



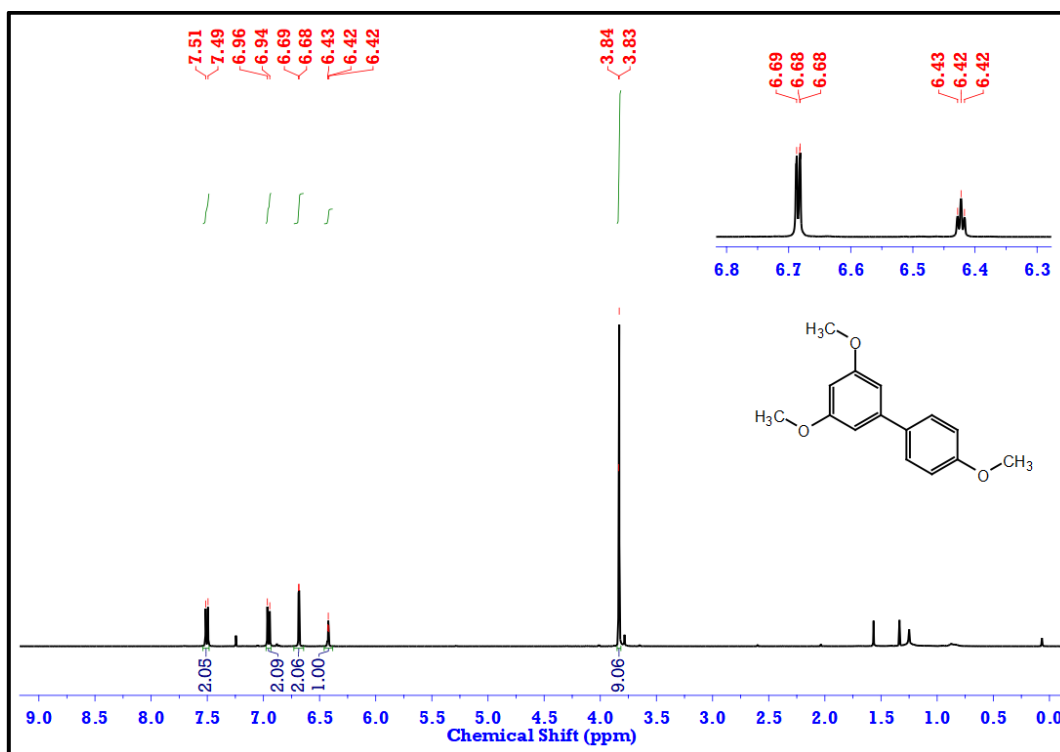
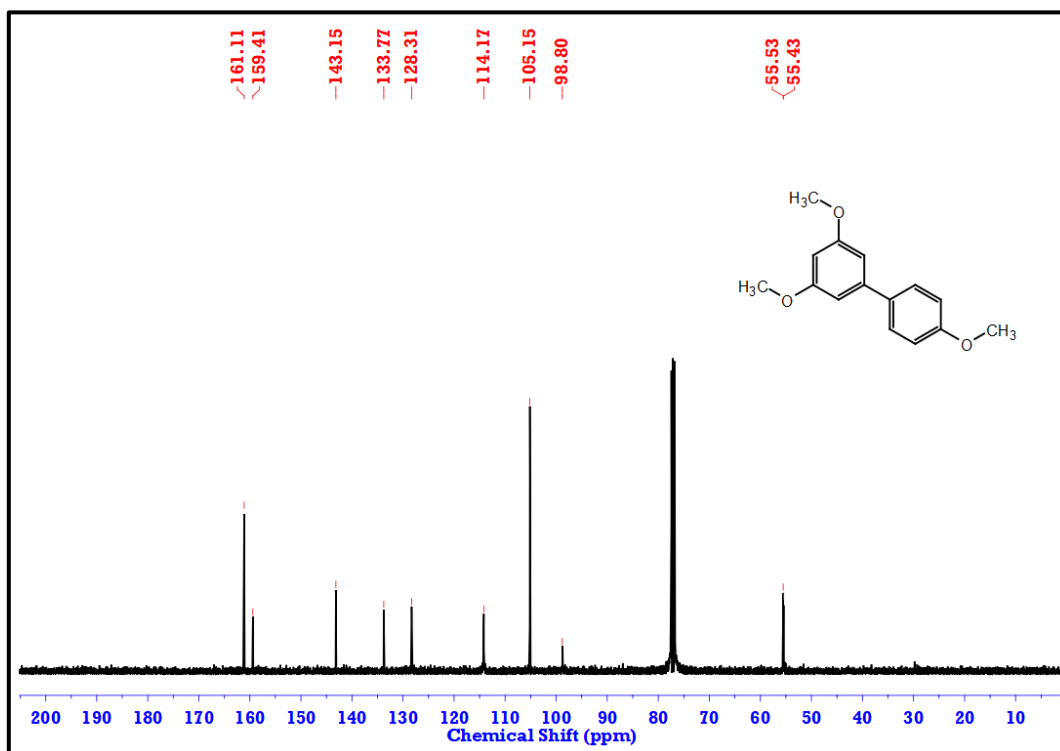
**5c. 3,4'-Dimethoxy-1,1'-biphenyl**, white solid:  $^1\text{H}$  NMR (500 MHz, CHLOROFORM-D)  $\delta$  (ppm) 7.52 (d,  $J = 8.7$  Hz, 2H), 7.32 (t,  $J = 7.9$  Hz, 1H), 7.17 – 7.07 (m, 2H), 6.97 (d,  $J = 8.7$  Hz, 2H), 6.85 (dd,  $J = 8.1, 2.3$  Hz, 1H), 3.85 (s, 3H), 3.84 (s, 3H).  $^{13}\text{C}$  NMR (125 MHz, CHLOROFORM-D)  $\delta$  (ppm) 160.0, 159.3, 142.4, 133.7, 129.7, 128.2, 119.3, 114.2, 112.6, 112.1, 55.4, 55.3.



**5d. 3,4,5-Trimethoxy-4'-chloro-1,1'-biphenyl**, white solid,  $^1\text{H}$  NMR (600 MHz, CHLOROFORM-D)  $\delta$  (ppm) 7.50 (d,  $J = 8.4$  Hz, 2H), 7.41 (d,  $J = 8.4$  Hz, 2H), 6.75 (s, 2H), 3.94 (s, 6H), 3.91 (s, 3H).  $^{13}\text{C}$  NMR (150 MHz, CHLOROFORM-D)  $\delta$  (ppm) 153.6, 139.8, 137.9, 136.0, 133.3, 128.9, 128.3, 104.3, 61.0, 56.2.



## 2.5. Representative NMR Spectra

**Figure 2.3.**  $^1\text{H}$  NMR Spectrum of 3a (3,4',5-Trimethoxy-1,1'-biphenyl) in  $\text{CDCl}_3$ **Figure 2.4.**  $^{13}\text{C}$  NMR Spectrum of 3a (3,4',5-Trimethoxy-1,1'-biphenyl) in  $\text{CDCl}_3$

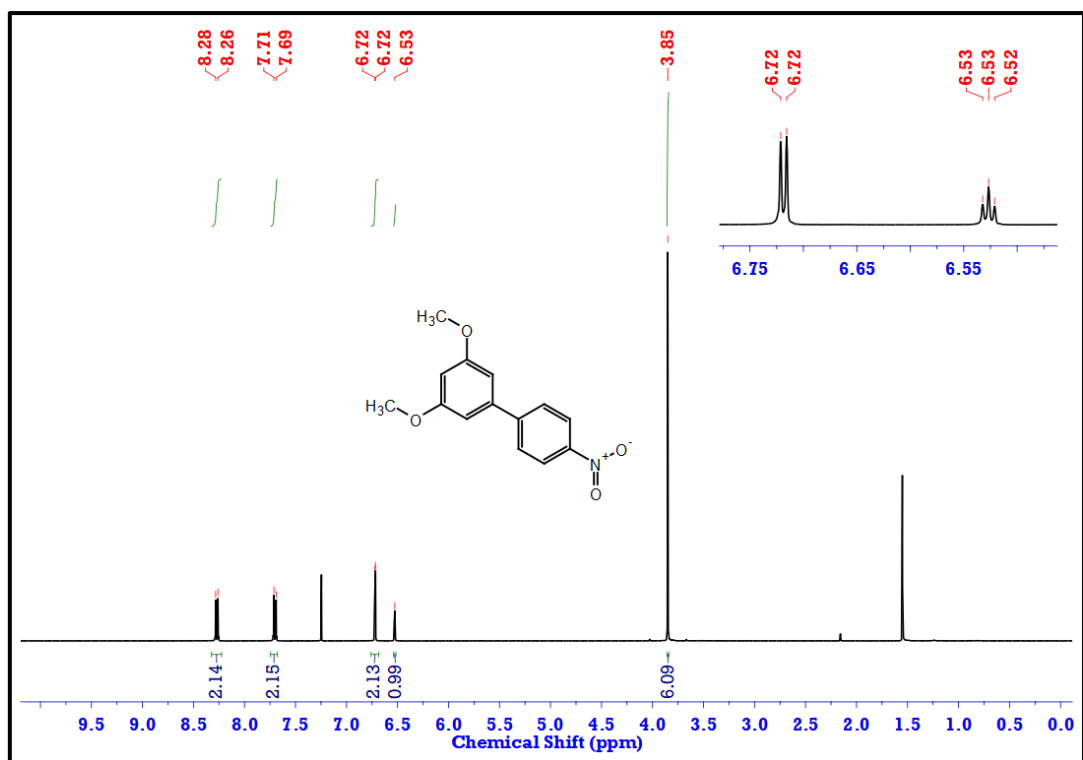


**Figure 2.5.** <sup>1</sup>H NMR Spectrum of 3d (3,5-dimethoxy-4'-nitro-1,1'-biphenyl) in CDCl<sub>3</sub>

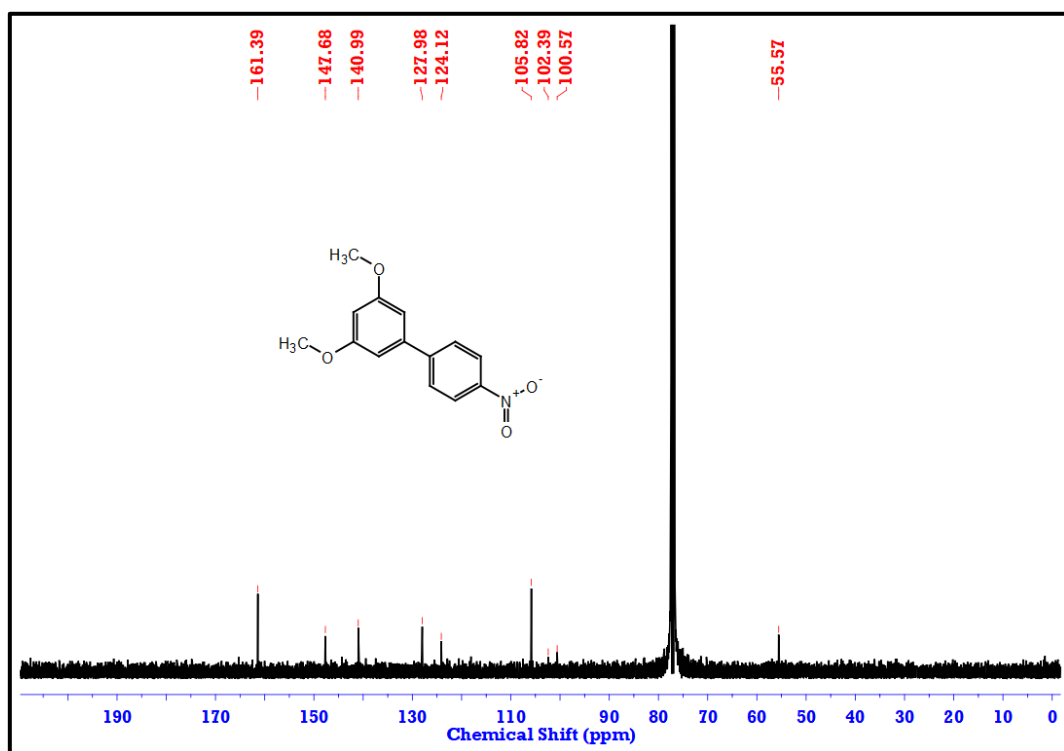


**Figure 2.6.** <sup>13</sup>C NMR Spectrum of 3d (3,5-dimethoxy-4'-nitro-1,1'-biphenyl) in CDCl<sub>3</sub>

### 2.6. Bibliography

- [1] Song, X., Zhang, Y., Ji, P., Zeng, F., Bi, F. and Wang, W. One-pot synthesis of salicylaldehyde containing biaryl frameworks *via* an aminocatalytic Diels-Alder-retro-Diels-Alder cascade reaction of ynals with 2-pyrones. *Green Synthesis and Catalysis*, 1(1):66-69, 2020.
- [2] Hassan, J., Sévignon, M., Gozzi, C., Schulz, E. and Lemaire, M. Aryl- aryl bond formation one century after the discovery of the Ullmann reaction. *Chemical Reviews*, 102(5):1359-1470, 2002.
- [3] Seregin, I.V. and Gevorgyan, V. Direct transition metal-catalysed functionalisation of heteroaromatic compounds. *Chemical Society Reviews*, 36(7):1173-1193, 2007.
- [4] Caron, L., Campeau, L.C. and Fagnou, K. Palladium-catalysed direct arylation of nitro-substituted aromatics with aryl halides. *Organic Letters*, 10(20):4533-4536, 2008.
- [5] Joucla, L. and Djakovitch, L. Transition Metal-Catalysed, Direct and Site-Selective N1-, C2-or C3-Arylation of the Indole Nucleus: 20 Years of Improvements. *Advanced Synthesis & Catalysis*, 351(5):673-714, 2009.
- [6] Loxq, P., Manoury, E., Poli, R., Deydier, E. and Labande, A. Synthesis of axially chiral biaryl compounds by asymmetric catalytic reactions with transition metals. *Coordination Chemistry Reviews*, 308:131-190, 2016
- [7] Corbet, J.P. and Mignani, G. Selected patented cross-coupling reaction technologies. *Chemical Reviews*, 106(7):2651-2710, 2006
- [8] Torborg, C. and Beller, M. Recent applications of palladium-catalysed coupling reactions in the pharmaceutical, agrochemical, and fine chemical industries. *Advanced Synthesis & Catalysis*, 351(18):3027-3043, 2009.
- [9] Hudrlik, P.F., Arasho, W.D. and Hudrlik, A.M. The Wurtz- Fittig Reaction in the Preparation of C-Silylated Calixarenes. *The Journal of Organic Chemistry*, 72(21):8107-8110, 2007.
- [10] Alberico, D., Scott, M.E. and Lautens, M. Aryl- aryl bond formation by transition-metal-catalysed direct arylation. *Chemical Reviews*, 107(1):174-238, 2007.

- [11] Konwar, D. and Bora, U. Recent Developments in Transition-Metal-Catalysed Regioselective Functionalisation of Imidazo [1, 2-a] pyridine. *ChemistrySelect*, 6(11):2716-2744, 2021.
- [12] Phipps, R.J. and Gaunt, M.J. A meta-selective copper-catalysed C–H bond arylation. *Science*, 323(5921):1593-1597, 2009.
- [13] Hofmann, N. and Ackermann, L. meta-Selective C–H bond alkylation with secondary alkyl halides. *Journal of the American Chemical Society*, 135(15):5877-5884, 2013.
- [14] Duong, H.A., Gilligan, R.E., Cooke, M.L., Phipps, R.J. and Gaunt, M.J. Copper (II)-Catalysed meta-Selective Direct Arylation of  $\alpha$ -Aryl Carbonyl Compounds. *Angewandte Chemie International Edition*, 123(2):483-486, 2011.
- [15] Saidi, O., Marafie, J., Ledger, A.E., Liu, P.M., Mahon, M.F., Kociok-Köhn, G., Whittlesey, M.K. and Frost, C.G. Ruthenium-catalysed meta sulfonation of 2-phenylpyridines. *Journal of the American Chemical Society*, 133(48):19298-19301, 2011.
- [16] Wan, L., Dastbaravardeh, N., Li, G. and Yu, J.Q. Cross-coupling of remote meta-C–H bonds directed by a U-shaped template. *Journal of the American Chemical Society*, 135(48):18056-18059, 2013.
- [17] Provencher, P.A., Bay, K.L., Hoskin, J.F., Houk, K.N., Yu, J.Q. and Sorensen, E.J. Cyclisation by C (sp<sup>3</sup>)–H arylation with a transient directing group for the diastereoselective preparation of indanes. *ACS Catalysis*, 11(5):3115-3127, 2021.
- [18] He, Y., Cai, Y. and Zhu, S. Mild and regioselective benzylic C–H functionalisation: Ni-catalysed reductive arylation of remote and proximal olefins. *Journal of the American Chemical Society*, 139(3):1061-1064, 2017.
- [19] Sinha, S.K., Guin, S., Maiti, S., Biswas, J.P., Porey, S. and Maiti, D. Toolbox for distal C–H bond functionalisations in organic molecules. *Chemical Reviews*, 122(6):5682-5841, 2021.
- [20] Dutta, U., Maiti, S., Bhattacharya, T. and Maiti, D. Arene diversification through distal C (sp<sup>2</sup>)– H functionalisation. *Science*, 372(6543):eabd5992, 2021.

- [21] Cornella, J., Righi, M. and Larrosa, I. Carboxylic acids as traceless directing groups for formal meta-selective direct arylation. *Angewandte Chemie International Edition*, 40(123):9601-9604, 2011.
- [22] Luo, J., Preciado, S., Araromi, S.O. and Larrosa, I. A Domino Oxidation/Arylation/Protodecarboxylation Reaction of Salicylaldehydes: Expanded Access to meta-Arylphenols. *Chemistry–An Asian Journal*, 11(3):347-350, 2016.
- [23] Pu, F., Zhang, L.Y., Liu, Z.W. and Shi, X.Y. Palladium (II)-Catalysed Decarboxylative Cross-Dehydrogenative Coupling: Direct Synthesis of meta-Substituted Biaryls from Aromatic Acids. *Advanced Synthesis & Catalysis*, 360(14):2644-2649, 2018.
- [24] Chiong, H.A., Pham, Q.N. and Daugulis, O. Two methods for direct *ortho*-arylation of benzoic acids. *Journal of the American Chemical Society*, 129(32):9879-9884, 2007.
- [25] Biafora, A., Krause, T., Hackenberger, D., Belitz, F. and Gooßen, L.J., 2016. *ortho*-C–H Arylation of Benzoic Acids with Aryl Bromides and Chlorides Catalysed by Ruthenium. *Angewandte Chemie International Edition*, 55(47):14752-14755, 2016.
- [26] Zhu, C., Zhang, Y., Kan, J., Zhao, H. and Su, W. Ambient-temperature *ortho* C–H arylation of benzoic acids with aryl iodides with ligand-supported palladium catalyst. *Organic Letters*, 17(14):3418-3421, 2015.
- [27] Zhao, Y. and Truhlar, D.G. The M06 suite of density functionals for main group thermochemistry, thermochemical kinetics, noncovalent interactions, excited states, and transition elements: two new functionals and systematic testing of four M06-class functionals and 12 other functionals. *Theoretical chemistry accounts*, 120:215-241, 2008.
- [28] Gaussian 16, Revision B.01, Frisch, M. J.; Trucks, G. W.; Schlegel, H. B.; Scuseria, G. E.; Robb, M. A.; Cheeseman, J. R.; Scalmani, G.; Barone, V.; Petersson, G. A.; Nakatsuji, H.; Li, X.; Caricato, M.; Marenich, A. V.; Bloino, J.; Janesko, B. G.; Gomperts, R.; Mennucci, B.; Hratchian, H. P.; Ortiz, J. V.; Izmaylov, A. F.; Sonnenberg, J. L.; Williams-Young, D.; Ding, F.; Lipparini, F.; Egidi, F.; Goings, J.; Peng, B.; Petrone, A.; Henderson, T.; Ranasinghe, D.; Zakrzewski, V. G.; Gao, J.; Rega, N.; Zheng, G.; Liang, W.; Hada, M.; Ehara, M.; Toyota, K.; Fukuda, R.; Hasegawa, J.; Ishida, M.; Nakajima, T.; Honda, Y.; Kitao, O.; Nakai, H.; Vreven, T.; Throssell, K.; Montgomery, Jr., J. A.; Peralta, J. E.; Ogliaro,

F.; Bearpark, M. J.; Heyd, J. J.; Brothers, E. N.; Kudin, K. N.; Staroverov, V. N.; Keith, T. A.; Kobayashi, R.; Normand, J.; Raghavachari, K.; Rendell, A. P.; Burant, J. C.; Iyengar, S. S.; Tomasi, J.; Cossi, M.; Millam, J. M.; Klene, M.; Adamo, C.; Cammi, R.; Ochterski, J. W.; Martin, R. L.; Morokuma, K.; Farkas, O.; Foresman, J. B. and Fox, D. J. Gaussian, Inc., Wallingford CT, 2016.

[29] Farrugia, L.J. WinGX and ORTEP for Windows: an update. *Journal of Applied Crystallography*, 45(4):849-854, 2012.